Development of a dynamic model for the subfilter scalar variance using the concept of optimal estimators

G. Balarac,[1] H. Pitsch,[1] and V. Raman[2]
[1]*Center for Turbulence Research, Stanford University, California 94305, USA*
[2]*The University of Texas at Austin, Austin, Texas 78712, USA*

(Received 11 January 2008; accepted 14 February 2008; published online 31 March 2008)

The concept of optimal estimators, recently introduced by Moreau *et al.* [Phys. Fluids **18**, 1 (2006)] is used as an *a priori* tool to discuss the accuracy of subfilter models. Placed in the framework of large-eddy simulation of combustion problems, this work focuses on the subfilter models used to evaluate the subfilter variance of a conserved scalar, the mixture fraction. The *a priori* tests are performed using 512^3 direct numerical simulation data of forced homogeneous isotropic turbulence. First, the performance of the most commonly used models for the subfilter variance is studied. Using optimal estimators, the Smagorinsky-type model [Pierce and Moin, Phys. Fluids **10**, 3041 (1998)] is shown to have the best set of parameters. However, the conventional dynamic formulation of the model leads to large errors in the variance prediction. It was found that assumptions used in the model formulation are not verified. A new dynamic procedure based on a Taylor series expansion is then proposed to improve the predictive accuracy. The *a priori* tests show that the new model substantially improves predictive accuracy. © *2008 American Institute of Physics*.
[DOI: 10.1063/1.2896287]

I. INTRODUCTION

Large-eddy simulation (LES) is based on the separation of turbulence scales into resolvable large scales and modeled small scales. A filtering operation,

$$\bar{f}(\vec{x},t) = \int f(\vec{y},t)\Phi(\vec{x}-\vec{y})d\vec{y}, \tag{1}$$

is used to obtain the large-scale resolved field, where $\bar{f}$ is the filtered field corresponding to a turbulent field f and Φ is the filter kernel. LES has been very successful in predicting free-shear flows since these flows are typically controlled by large-scale energy containing motions.[1–3] Several models for the subfilter unresolved terms have been proposed in this context.[4] While the LES formulation is useful in such flows, combustion or wall-bounded flows are controlled by the small-scale evolution of the turbulence and are not naturally described by the large scales. Consequently, detailed subfilter modeling in combustion is very critical in ensuring predictive accuracy. Interestingly, the ability of LES to describe large-scale scalar mixing provides a natural starting point for modeling turbulence-chemistry interactions at the small scales. In this context, the purpose of this work is to assess the predictive accuracy of currently used models and provide improved formulations.

LES of turbulent combustion often employs conserved scalar based formulations.[5] The mixture fraction Z is a conserved scalar that is used to describe the local thermochemical state of the fluid. To obtain the filtered thermochemical vector, the subfilter distribution of mixture fraction is required. Since LES resolves only the large scales, this information needs to be provided through a statistical description of the subfilter state. Typically, a presumed probability density function (PDF) in the form of a beta function is used.[6] The PDF is parametrized by the filtered mixture fraction $\bar{Z}$ and the mixture-fraction variance, $Z_v = \overline{ZZ} - \bar{Z}\bar{Z}$. Since the subfilter variance is not directly available in LES, several models have been proposed for this quantity. The performance of these models is often not of satisfactory accuracy given their importance for predicting the heat release and the effect of the heat release on the large-scale motion of the flow.

In this work, we first study the performance of the most commonly used models, namely, the scale-similarity model[6] and the dynamic Smagorinsky-type model.[7] The validity of the assumptions used to construct the dynamic Smagorinsky-type model is tested. To improve the predictive accuracy, a new dynamic procedure based on a Taylor series expansion is then proposed. The new model is examined in *a priori* tests and compared with the dynamic Smagorinsky-type model.

II. NUMERICAL METHOD

In this work, *a priori* tests are conducted using direct numerical simulation (DNS) data from a forced homogeneous isotropic turbulence computation. A pseudospectral code with second-order explicit Runge–Kutta time advancement is used. The viscous terms are treated exactly. The simulation domain is discretized using 512^3 grid points on a domain of length 2π. A classic $\frac{3}{2}$ rule is used for dealiasing the nonlinear convection term, and statistical stationarity is achieved using a forcing term.[8] The mixture-fraction equation is advanced simultaneously using an identical numerical scheme. To enforce stationarity of the scalar field, a mean scalar gradient is imposed.[9] The size of the computational domain is larger than four times the integral length scale to ensure that the largest flow structures are not affected. The simulation parameters are chosen such that $k_{\max}\eta > 1.5$ and $k_{\max}\eta_B > 1.5$, where $k_{\max}$ is the maximum wavenumber in the

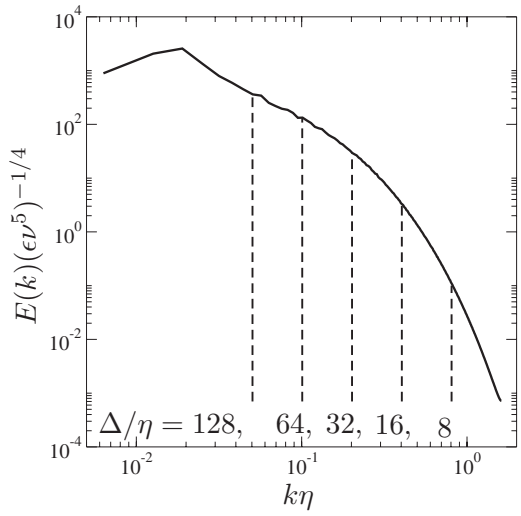

FIG. 1. Kinetic energy spectrum with the location of filters used in this work.

domain, and η and η_B are the Kolmogorov and Batchelor scales, respectively. The Reynolds number based on the Taylor microscale is around 180 and the molecular Schmidt number is set to 0.7. The numerical implementation has been verified by comparing the skewness and flatness of the velocity derivative with Jimenez and Wray[10] for similar Reynolds numbers.

In the *a priori* tests, the box filter is used to replicate the behavior of the filter implicitly associated with the discretization using centered finite differences often used in LESs of engineering flows.[1] Several different filter sizes have been used, chosen as $\Delta/\Delta x$=2, 4, 8, 16, and 32, where Δ is the filter width and Δx is the grid spacing used in the DNS. This corresponds to $\Delta/\eta \approx 8$, 16, 32, 64, and 128, where, according to Pope,[4] the latter two are in the inertial subrange. The location in wavenumber space of the filters used are displayed in Figs. 1 and 2, which show the kinetic energy and scalar variance spectra.

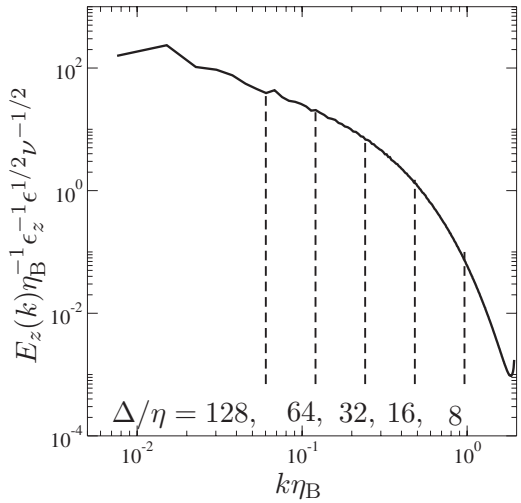

FIG. 2. Scalar variance spectrum with the location of filters used in this work.

III. PREVIOUS SUBFILTER SCALAR VARIANCE MODELS

Several models for the subfilter variance have been proposed in the past.[6,7] The scale-similarity model[6] uses the self-similar behavior of turbulent properties at different length scales to model the subfilter variance. The scalar variance is then written as

$$Z_{v,\mathrm{SS}} = C_s(\widehat{\hat{Z}\hat{Z}} - \hat{\bar{Z}}\hat{\bar{Z}}). \tag{2}$$

In this equation, $\hat{\cdot}$ denotes a test filter and C_s is the scale-similarity constant that needs to be specified. C_s is highly flow dependent and is not a universal constant. Hence, *a priori* specification almost always introduces large errors.[11] Pierce and Moin[7] proposed a dynamic formulation that is based on a mixing length hypothesis similar to the Smagorinsky model. In this approach, the model constant is evaluated as a varying parameter using the filtered fields available in LES. A scalar-gradient-based scaling law is used to obtain a closed-form algebraic equation for the subfilter variance,

$$Z_{v,\mathrm{DM}} = C_d\Delta^2\frac{\partial\bar{Z}}{\partial x_i}\frac{\partial\bar{Z}}{\partial x_i}, \tag{3}$$

where C_d is the model constant that is determined dynamically. Assuming that the model coefficient varies slowly in space and that the same coefficient applies both at the filter level and a larger test filter level, Eq. (3) can be written at the filter level and then filtered again at the test filter level leading to

$$\widehat{\bar{Z}\bar{Z}} - \hat{\bar{Z}}\hat{\bar{Z}} = C_d\Delta^2\widehat{\frac{\partial\bar{Z}}{\partial x_i}\frac{\partial\bar{Z}}{\partial x_i}} \tag{4}$$

or it can be written at the test filter level, which gives

$$\widehat{\bar{Z}\bar{Z}} - \hat{\bar{Z}}\hat{\bar{Z}} = C_d\hat{\Delta}^2\frac{\partial\hat{\bar{Z}}}{\partial x_i}\frac{\partial\hat{\bar{Z}}}{\partial x_i}, \tag{5}$$

where $\hat{\Delta}$ is the test filter width. In the present paper, $\hat{\Delta}=2\Delta$ will be used. Subtracting Eq. (4) from Eq. (5) then provides

$$L_d = C_d M_d, \tag{6}$$

with

$$L_d = \widehat{\hat{Z}\hat{Z}} - \hat{\bar{Z}}\hat{\bar{Z}}$$

and

$$M_d = \hat{\Delta}^2\frac{\partial\hat{\bar{Z}}}{\partial x_i}\frac{\partial\hat{\bar{Z}}}{\partial x_i} - \Delta^2\widehat{\frac{\partial\bar{Z}}{\partial x_i}\frac{\partial\bar{Z}}{\partial x_i}}.$$

Assuming that the coefficient is constant over homogeneous directions, C_d is then obtained using a least-squares averaging procedure

$$C_d = \frac{\langle L_d M_d \rangle}{\langle M_d M_d \rangle}, \tag{7}$$

where the brackets indicate averaging over homogeneous directions. Note that in the case of homogeneous turbulence, C_d is constant in all the domains.

As a first step toward understanding modeling errors, both these models were evaluated *a priori* using DNS data. For these tests, the scale-similarity constant was taken to be equal to unity.[6] In the framework of optimal estimation theory,[12] the models are compared using the notion of an optimal estimator.[13] Based on this idea, if a quantity Z_v is modeled with a finite set of variables ϕ, an exact model cannot be guaranteed. If the exact solution Z_v is known, for example, from DNS, the optimal estimator of Z_v in terms of the set of variables ϕ is given by the expectation of the quantity Z_v conditioned on the variables in the set. A quadratic error can consequently be defined as the average of the square of the difference at each point between the conditional mean value given by the value of ϕ at this point and the exact value of the quantity,

$$\epsilon_{\min} = \langle (Z_v - \langle Z_v | \phi \rangle)^2 \rangle, \tag{8}$$

where $\epsilon_{\min}$ is the error and the angular brackets indicate statistical averaging over a suitable ensemble. It should be noted that any model formulated using the variable set ϕ will introduce an error that is larger than or equal to this minimum error, with the best model formulation producing this minimum error. Consequently, this quadratic error $\epsilon_{\min}$ is referred to as the irreducible error. Only a change in the variable set may reduce the magnitude of this error. In contrast, the total quadratic error is given as

$$\epsilon_{\text{tot}} = \langle (Z_v - Z_{v,\text{model}})^2 \rangle. \tag{9}$$

For the dynamic Smagorinsky-type model, the variable set used is $\phi_1 = \{(\partial \bar{Z}/\partial x_i)(\partial \bar{Z}/\partial x_i)\}$, whereas the variable set for the scale-similarity model is $\phi_2 = \{\widehat{\bar{Z}\bar{Z}} - \hat{\bar{Z}}\hat{\bar{Z}}\}$. Note that the variables used to define C_d in the dynamic formulation are not taken into account since C_d is constant due to the averaging process. Figure 3 shows the total quadratic errors of the scale-similarity and dynamic Smagorinsky-type models as a function of the filter width. The irreducible errors associated with the corresponding variable sets are also shown. The errors have been normalized by the square of the exact subfilter variance expectation. When the filter is located in the inertial-convective range of the scalar spectrum, the quadratic errors of each model begin to be significantly larger than their associated irreducible errors. This is particularly true for the dynamic Smagorinsky-type model showing a very large error compared with the irreducible error for large filter size. However, if only the irreducible errors are compared, it is noticed that the irreducible error corresponding to the dynamic Smagorinsky-type model is always lower than the irreducible error corresponding to the scale-similarity model. These results show that a better model can potentially be formulated with the variable set ϕ_1 than for variable set ϕ_2, but that a substantial improvement is needed to achieve this goal.

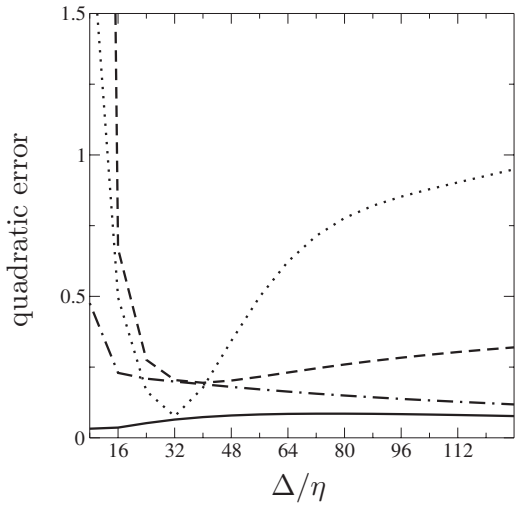

FIG. 3. Evolution of the total quadratic errors of the scale-similarity and dynamic Smagorinsky-type models and their associated irreducible error with the filter width. The errors have been normalized by the square of the exact subfilter variance expectation. $\langle (Z_v - \langle Z_v | \phi_1 \rangle)^2 \rangle / \langle Z_v \rangle^2$ (—), $\langle (Z_v - Z_{v,\text{DM}})^2 \rangle / \langle Z_v \rangle^2$ (···), $\langle (Z_v - \langle Z_v | \phi_2 \rangle)^2 \rangle / \langle Z_v \rangle^2$ (–·–), and $\langle (Z_v - Z_{v,\text{SS}})^2 \rangle / \langle Z_v \rangle^2$ (----).

While the dynamic Smagorinsky-type model produces a large total quadratic error, the variable set corresponding to this model produces a relatively small irreducible error. This means that the assumptions that lead to the functional form of the model formulation introduce the errors observed in the *a priori* tests. To understand the source of these errors, the main assumptions that lead to the dynamic formulation are studied next. From Eqs. (3)–(6), the quantities C_1, C_2, C_3, and C_4 are defined from the DNS data as

$$\overline{ZZ} - \bar{Z}\bar{Z} = C_1 \Delta^2 \frac{\partial \bar{Z}}{\partial x_i} \frac{\partial \bar{Z}}{\partial x_i}, \tag{10}$$

$$\widehat{\bar{Z}\bar{Z}} - \hat{\bar{Z}}\hat{\bar{Z}} = C_2 \Delta^2 \widehat{\frac{\partial \bar{Z}}{\partial x_i} \frac{\partial \bar{Z}}{\partial x_i}}, \tag{11}$$

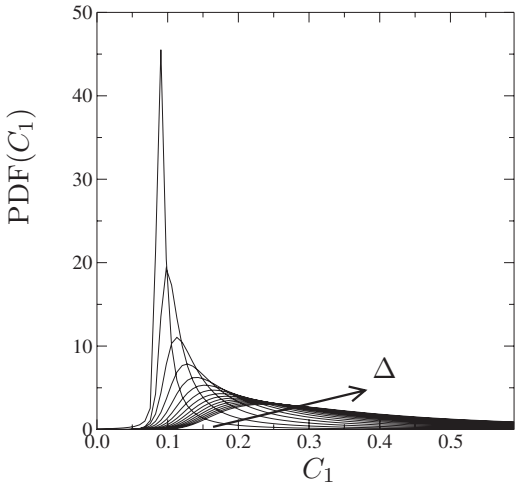

FIG. 4. PDF of C_1 [Eq. (10)] for several filter sizes. The arrow indicates increasing filter size.

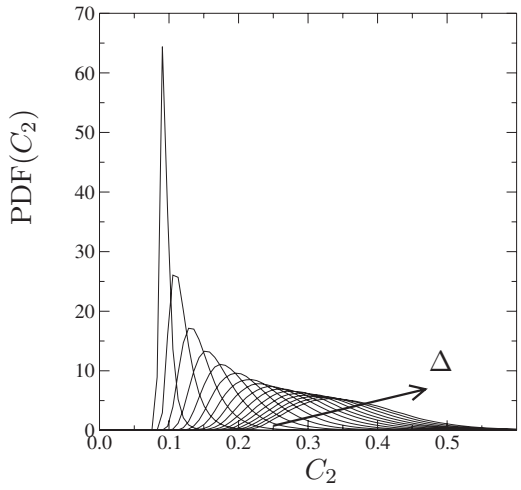

FIG. 5. PDF of C_2 [Eq. (11)] for several filter sizes. The arrow indicates increasing filter size.

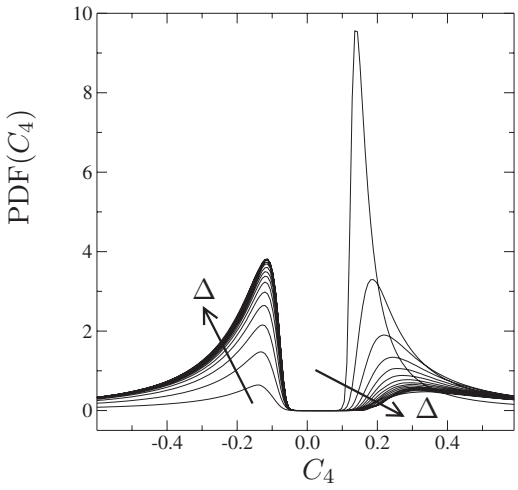

FIG. 7. PDF of C_4 [Eq. (13)] for several filter sizes. The arrow indicates increasing filter size.

$$\widehat{\overline{Z}\overline{Z}} - \hat{\overline{Z}}\hat{\overline{Z}} = C_3\hat{\Delta}^2\frac{\partial\hat{\overline{Z}}}{\partial x_i}\frac{\partial\hat{\overline{Z}}}{\partial x_i}, \tag{12}$$

and

$$\widehat{\overline{Z}\overline{Z}} - \hat{\overline{Z}}\hat{\overline{Z}} = C_4\left(\hat{\Delta}^2\frac{\partial\hat{\overline{Z}}}{\partial x_i}\frac{\partial\hat{\overline{Z}}}{\partial x_i} - \Delta^2\widehat{\frac{\partial\overline{Z}}{\partial x_i}\frac{\partial\overline{Z}}{\partial x_i}}\right). \tag{13}$$

Note that these quantities are spatially varying. The main modeling hypothesis of the dynamic Smagorinsky-type model is to assume that C_1, C_2, and C_3 are constant over homogeneous directions and equal to C_d. This assumption also requires C_4 to be constant over homogeneous directions and to be equal to C_d. Figures 4–6 show the probability PDFs of C_1, C_2, and C_3 for several filter sizes. The coefficients C_1 and C_2 have clearly unimodal distributions with distinct peaks, particularly for small filter sizes. This validates the assumption of constant quantities. The distribution of C_1 shows that the model (3) is valid but also that the model coefficient is far from universal, even in such simple flows, and that a dynamic procedure is required to improve predictive accuracy. The coefficient C_3, however, has a broad distribution even for small filter sizes, showing that a constant value of C_3 cannot be assumed. Moreover, the ranges of values of C_1, C_2, and C_3 are clearly different. The assumption $C_1=C_2=C_3=C_d$ is thus not verified. In this case, the equality $C_4=C_d$ used to compute the dynamic constant cannot be true. Indeed, C_4 clearly has a bimodal distribution and cannot be assumed to be constant (Fig. 7). Note that C_4 contains a large negative range that would lead to negative, and hence unrealizable, variance. The reasons for these findings will be further discussed below. Both the unphysical behavior and the scale dependence of the model coefficients need to be addressed. In this context, a new model formulation is discussed next.

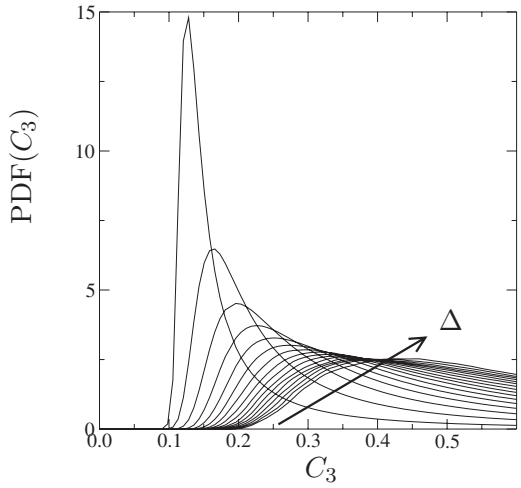

FIG. 6. PDF of C_3 [Eq. (12)] for several filter sizes. The arrow indicates increasing filter size.

IV. SUBFILTER SCALAR VARIANCE MODELING BASED ON TAYLOR SERIES

The starting point for a new subfilter scalar variance model is based on a Taylor series expansion. This approach has already been used by several authors[14,15] to derive the so-called Clark's gradient model. Here, we briefly describe the method proposed by Bedford and Yeo[16] to give an expansion for $\overline{fg}$ as a function of f and $\bar{g}$ and their derivatives (where f and g are quantities describing flow fields).

A. Bedford and Yeo's expansion

Bedford and Yeo[16] proposed an expansion of $\overline{fg}$ based on Taylor series in the case of a Gaussian filter. The starting point is that in spectral space, the filtering operation (1) is

$$\check{f}(\vec{k}) = \check{f}(\vec{k})\check{\Phi}(\vec{k}), \tag{14}$$

where $\check{f}(\vec{k})$ is the Fourier transform of $f(\vec{x})$ and $\vec{k}$ is the wavevector. The Taylor series of a Gaussian filter of the form $\check{\Phi}(\vec{k})=\exp(-\Delta^2k^2/24)$ is given as

$$\check{\Phi}(\vec{k}) = 1 - \frac{\Delta^2}{24}k^2 + \frac{\Delta^4}{1152}k^4 - \frac{\Delta^6}{82\,944}k^6 + \cdots . \tag{15}$$

Since the Laplacian operator, $L(f) = \partial^2 f / \partial x_i^2$, is given in spectral space by

$$\check{L}(f) = -k^2 \check{f}(\vec{k}), \tag{16}$$

the inverse Fourier transform of Eq. (14) combined with Eq. (15) yields for the filtered function in physical space,

$$\overline{f} = f + \frac{\Delta^2}{24}L(f) + \frac{\Delta^4}{1152}L^{(2)}(f) + \frac{\Delta^6}{82\,944}L^{(3)}(f) + \cdots , \tag{17}$$

where $L^{(n)}$ is the Laplacian operator applied n times. Moreover, in spectral space, we can write the filtering operation as

$$\check{f}(\vec{k}) = \frac{1}{\Phi(\vec{k})}\check{\overline{f}}(\vec{k}). \tag{18}$$

We can then write a Taylor series for $1/\check{\Phi}(\vec{k}) = \exp(\Delta^2 k^2/24)$ as

$$1/\check{\Phi}(\vec{k}) = 1 + \frac{\Delta^2}{24}k^2 + \frac{\Delta^4}{1152}k^4 + \frac{\Delta^6}{82\,944}k^6 + \cdots , \tag{19}$$

which leads to

$$f = \overline{f} - \frac{\Delta^2}{24}L(\overline{f}) + \frac{\Delta^4}{1152}L^{(2)}(\overline{f}) - \frac{\Delta^6}{82\,944}L^{(3)}(\overline{f}) + \cdots . \tag{20}$$

Considering the expansion (17) for $\overline{fg}$, after substitution of f and g by their expansion (20), and after considerable algebra, Bedford and Yeo[16] found the expansion

$$\overline{fg} = \overline{f}\,\overline{g} + \frac{\Delta^2}{12}\frac{\partial \overline{f}}{\partial x_i}\frac{\partial \overline{g}}{\partial x_i} + \frac{\Delta^4}{288}\frac{\partial^2 \overline{f}}{\partial x_i \partial x_j}\frac{\partial^2 \overline{g}}{\partial x_i \partial x_j} + \frac{\Delta^6}{10\,368}\frac{\partial^3 \overline{f}}{\partial x_i \partial x_j \partial x_k}\frac{\partial^3 \overline{g}}{\partial x_i \partial x_j \partial x_k} + \cdots . \tag{21}$$

Note that this expansion is based on the Gaussian filter and is not valid for other filters. Similar results have been derived elsewhere for the subfilter kinetic energy.[17] Moreover, if $f = u_i$ and $g = u_j$, and if only the first two terms of the right-hand side (RHS) are considered, the gradient model proposed by Clark *et al.*[14] to model the subfilter stress tensor is obtained. The Clark's relation can be used to model different types of subfilter terms as long as the modeled terms have the most part of their energy at large scales because, otherwise, the truncation error of the expansion will be too large. For instance, da Silva and Pereira[18] have recently modeled successfully the subfilter pressure-velocity term in the transport equation of the subfilter kinetic energy using this relation.

B. Subfilter scalar variance modeling: New dynamic procedure

Before deriving a new dynamic procedure, the dynamic Smagorinsky-type model assumptions can be examined in the light of expansion (21). We will start by deriving Eq. (5) from Eq. (21), which is the Smagorinsky-type model at the test filter scale. Note that in the derivation of the dynamic model, it is assumed that test-filtered quantities such as $\hat{\overline{Z}}$ are obtained by first applying the filter on the regular scale and then applying the filter on the test-filter scale. Because of this, the modeling assumption used for Eq. (5) is not the same as that in Eq. (3). In fact, Eq. (3) follows from the mixing length assumption, whereas the model used in Eq. (5) would actually be the mixing length expression for $\widehat{\overline{Z}\overline{Z}} - \hat{\overline{Z}}\hat{\overline{Z}}$. Using the expression (21) to expand $\widehat{\overline{Z}\overline{Z}}$ leads to

$$\widehat{\overline{Z}\overline{Z}} = \widehat{\overline{Z}}\,\widehat{\overline{Z}} + \frac{\Delta^2}{12}\widehat{\frac{\partial \overline{Z}}{\partial x_i}\frac{\partial \overline{Z}}{\partial x_i}} + \cdots$$

$$= \hat{\overline{Z}}\hat{\overline{Z}} + \frac{\hat{\Delta}^2}{12}\frac{\partial \hat{\overline{Z}}}{\partial x_i}\frac{\partial \hat{\overline{Z}}}{\partial x_i} + \frac{\Delta^2}{12}\widehat{\frac{\partial \overline{Z}}{\partial x_i}\frac{\partial \overline{Z}}{\partial x_i}} + \cdots . \tag{22}$$

Equation (22) shows that $\widehat{\overline{Z}\overline{Z}} - \hat{\overline{Z}}\hat{\overline{Z}}$ cannot be described by the term $\hat{\Delta}^2(\partial \hat{\overline{Z}}/\partial x_i)(\partial \hat{\overline{Z}}/\partial x_i)$ without taking the term $\Delta^2\widehat{(\partial \overline{Z}/\partial x_i)(\partial \overline{Z}/\partial x_i)}$ into account. This shows that the assumption (5) is incorrect, as discussed before, and already seen in the behavior of C_3. From this, follows that Eq. (6), which is deduced from Eq. (5), cannot be used for the formulation of the dynamic procedure, as already seen in the behavior of C_4.

For the subfilter scalar variance, the first order of the expansion (21) leads to the model

$$Z_{v,o2} = \frac{\Delta^2}{12}\frac{\partial \overline{Z}}{\partial x_i}\frac{\partial \overline{Z}}{\partial x_i}, \tag{23}$$

which is similar to the dynamic Smagorinsky-type model, but using $C_d = 1/12$ instead of computing C_d dynamically. One could use this constant value to compute the variance. However, since the higher-order terms of the expansion are discarded in this model, a dynamic coefficient, C_n, can be introduced to account for the truncation error. The new formulation can be written as

$$Z_{v,\mathrm{LED}} = C_n \Delta^2 \frac{\partial \overline{Z}}{\partial x_i}\frac{\partial \overline{Z}}{\partial x_i}. \tag{24}$$

Since the Leonard term, $\widehat{\overline{Z}\overline{Z}} - \hat{\overline{Z}}\hat{\overline{Z}}$, is available in LES, the Taylor series expansion of this term can be used to determine the dynamic coefficient. The expansion (21) is written for the test filter with $f = \overline{Z}$ and $g = \overline{Z}$. This leads to

$$\widehat{\overline{Z}\overline{Z}} - \hat{\overline{Z}}\hat{\overline{Z}} = \frac{\hat{\Delta}^2}{12}\frac{\partial \hat{\overline{Z}}}{\partial x_i}\frac{\partial \hat{\overline{Z}}}{\partial x_i} + \frac{\hat{\Delta}^4}{288}\frac{\partial^2 \hat{\overline{Z}}}{\partial x_i \partial x_j}\frac{\partial^2 \hat{\overline{Z}}}{\partial x_i \partial x_j} + \cdots . \tag{25}$$

Equation (25) shows that $\widehat{\overline{Z}\overline{Z}} - \hat{\overline{Z}}\hat{\overline{Z}}$ can be evaluated from the derivatives of $\hat{\overline{Z}}$, which are also available in LES. Here, we keep only the first order term of the RHS and introduce a dynamic coefficient to account for the truncation error. This

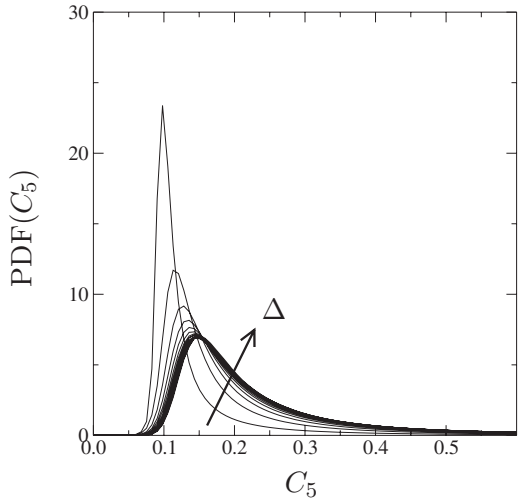

FIG. 8. PDF of C_5 [Eq. (26)] for several filter sizes. The arrow indicates increasing filter size.

coefficient is assumed to be equal to C_n, already used in Eq. (24).

To assess this assumption, a spatially dependent quantity C_5 is defined as

$$\widehat{\overline{Z}\overline{Z}} - \hat{\overline{Z}}\hat{\overline{Z}} = C_5\hat{\Delta}^2 \frac{\partial \hat{\overline{Z}}}{\partial x_i}\frac{\partial \hat{\overline{Z}}}{\partial x_i}. \tag{26}$$

The PDFs of C_5 for several filter sizes are shown in Fig. 8. The distribution of C_5 is unimodal with a distinct peak, as already seen with C_1. Moreover, the range of values of C_5 is close to the range of values of C_1. This confirms that the assumptions that C_1 and C_5 are constant over homogeneous directions and that $C_1=C_5=C_n$ are valid. Assuming that C_n is constant over homogeneous directions, a simple average yields

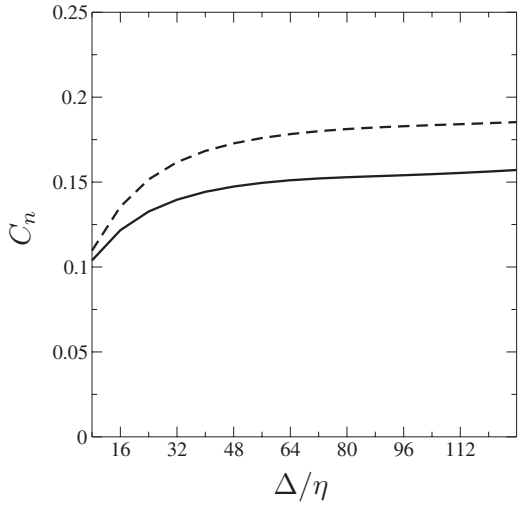

FIG. 9. Model constant computed following both ways given in Eqs. (27) and (28). $C_n=\langle L_n M_n\rangle/\langle M_n M_n\rangle$ (—) and $C_n=\langle L_n\rangle/\langle M_n\rangle$ (----).

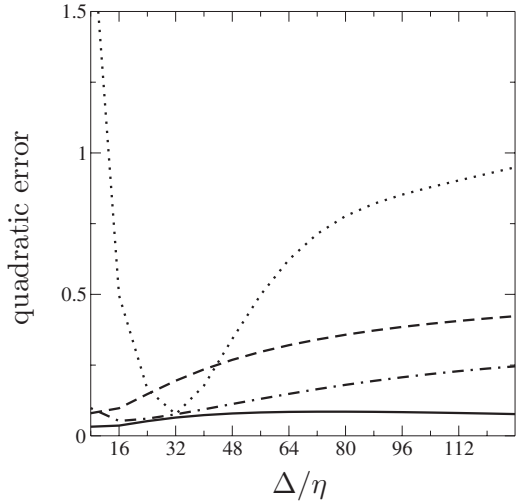

FIG. 10. Evolution of the total quadratic errors of the models $Z_{v,\mathrm{DM}}$, $Z_{v,\mathrm{o2}}$, and $Z_{v,\mathrm{LED}}$ and the associated irreducible error with the filter width. The errors have been normalized by the square of the exact subfilter variance expectation. $\langle(Z_v-\langle Z_v|\phi_1\rangle)^2\rangle/\langle Z_v\rangle^2$ (—), $\langle(Z_v-Z_{v,\mathrm{DM}})^2\rangle/\langle Z_v\rangle^2$ (···), $\langle(Z_v-Z_{v,\mathrm{o2}})^2\rangle/\langle Z_v\rangle^2$ (----), and $\langle(Z_v-Z_{v,\mathrm{LED}})^2\rangle/\langle Z_v\rangle^2$ (-·-·).

$$C_n = \frac{\langle L_n\rangle}{\langle M_n\rangle}, \tag{27}$$

with $L_n=\widehat{\overline{Z}\overline{Z}}-\hat{\overline{Z}}\hat{\overline{Z}}$ and $M_n=\hat{\Delta}^2(\partial\hat{\overline{Z}}/\partial x_i)(\partial\hat{\overline{Z}}/\partial x_i)$. Instead, C_n can also be evaluated from a least-squares approximation according to Lilly's method[19] as

$$C_n = \frac{\langle L_n M_n\rangle}{\langle M_n M_n\rangle}. \tag{28}$$

Figure 9 shows that both methods are close. In the following, C_n is computed with the least-squares averaging. Since this new dynamic procedure is based on a Taylor series expansion of the Leonard term, we will refer to this model as the *Leonard term expansion dynamic model* (LED).

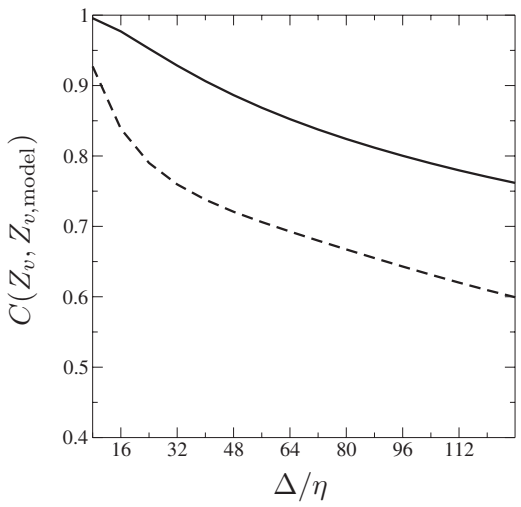

FIG. 11. Correlation between Z_v and $Z_{v,\mathrm{LED}}$ (—) and between Z_v and $Z_{v,\mathrm{SS}}$ (----).

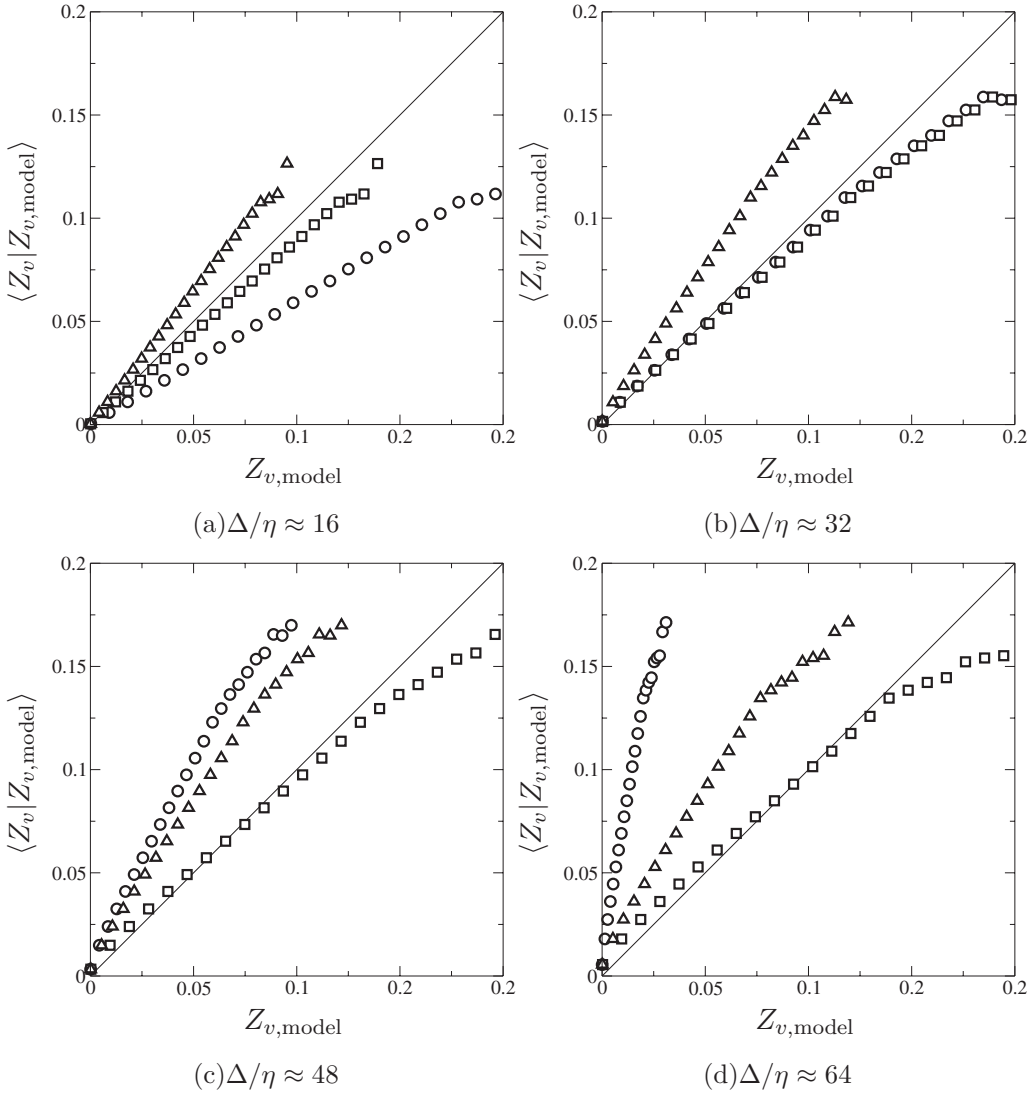

FIG. 12. Plot of $\langle Z_v | Z_{v,\mathrm{model}} \rangle$ as a function of $Z_{v,\mathrm{model}}$. $Z_{v,\mathrm{DM}}$ (○), $Z_{v,o2}$ (△), and $Z_{v,\mathrm{LED}}$ (□). $y=x$ (—).

C. *A priori* tests of LED model

The analyses in the previous sections were carried out using a Gaussian filter kernel. In practical LES calculations, only a box filter is used. Hence, to ensure that the model performance is not dependent on the filter kernel, *a priori* tests were conducted using the box filter. The box filter is applied by multiplication with the following kernel:

$$\check{\Phi}(\vec{k}) = \prod_{i=1}^{3} \frac{\sin(k_i \Delta/2)}{k_i \Delta/2}$$

in spectral space.

Figure 10 shows the quadratic errors for the different models. Note that the model $Z_{v,o2}$ given by Eq. (23) is also tested for comparison. For all filter sizes, the total quadratic error of $Z_{v,\mathrm{LED}}$ is smaller than the total quadratic errors obtained with the two other models. Moreover, the total quadratic error of the new dynamic procedure remains close to the irreducible error, whereas the total quadratic error of the dynamic Smagorinsky-type model increases strongly with the filter size. This shows that $Z_{v,\mathrm{LED}}$ is close to the best possible model using only ϕ_1 as variable set. We can also note that the total quadratic error of $Z_{v,\mathrm{LED}}$ is close to the irreducible error using ϕ_2 as set of quantities (Fig. 3). This shows that $Z_{v,\mathrm{LED}}$ will be more accurate than a scale-similarity model independent of the scale-similarity constant C_s. To confirm that it is better to use a gradient-type model than a scale-similarity model, Fig. 11 shows the correlation between the exact subfilter variance obtained from the DNS data and the modeled subfilter variance. It is evident that a gradient-type model is strongly correlated with the exact subfilter variance and that the correlation is higher than that of the scale-similarity model for all filter sizes.

To assess the quality of a model, a scatter plot showing the model result, $g(\phi)$, versus the modeled quantity, Z_v, is often used. In the same spirit, Moreau *et al.*[13] proposed to consider $\langle Z_v | g(\phi) \rangle$ as a function of $g(\phi)$, which compares the model results with the best possible model given a certain parameter set ϕ. They demonstrate that the model is optimal when $\langle Z_v | g(\phi) \rangle = g(\phi)$. Figure 12 shows $\langle Z_v | Z_{v,\mathrm{model}} \rangle = f(Z_{v,\mathrm{model}})$ for several filter sizes. For the dy-

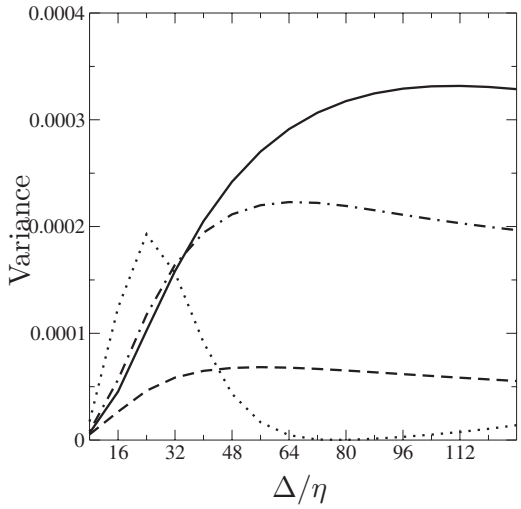

FIG. 13. Variance of the subfilter. Z_v (—), $Z_{v,\mathrm{DM}}$ (···), $Z_{v,\mathrm{o2}}$ (----), and $Z_{v,\mathrm{LED}}$ (–·–).

namic Smagorinsky-type model, the large total quadratic errors for large filter sizes are due to an important underprediction of the subfilter scalar variance. This underprediction is due to the large part of negative values of C_4, as previously observed. The model $Z_{v,\mathrm{o2}}$ always underpredicts the subfilter scalar variance due to the truncation error since all the terms of the expansion (21) are positive. For the LED model, there is just a weak overprediction of the high values of the subfilter scalar variance, but for most of the range of the scalar variance, the model is in excellent agreement with the data.

In LES, the subfilter variance itself is a fluctuating random quantity. Hence, all statistical measures used in the context of other random variables can be invoked for the variance as well. The variance, skewness, and flatness of the subfilter variance model are compared with the moments of the exact subfilter variance. These quantities define the moments of the PDF of the subfilter variance. Hence, they help compare the distribution given by the models with the exact distribution. Figure 13 shows the variance of the exact and modeled subfilter variances. We can see first that the underprediction of $Z_{v,\mathrm{o2}}$ leads to a smaller variance of the subfilter variance. The Smagorinsky-type model produces higher variance for small filter sizes, but the variance is nearly zero for large filter sizes. These underpredictions are mainly due to the large negative value of C_4 given by the model. The LED model underpredicts the variance of the subfilter quantity but still predicts the right trend. Figure 14 shows the skewness and the flatness of Z_v and $Z_{v,\mathrm{LED}}$. Note that these quantities are independent of the model coefficient. Again, a similar behavior between the model and the exact subfilter variance is found. All these observations indicate that the LED model reproduces the distribution of the subfilter variance with reasonable accuracy.

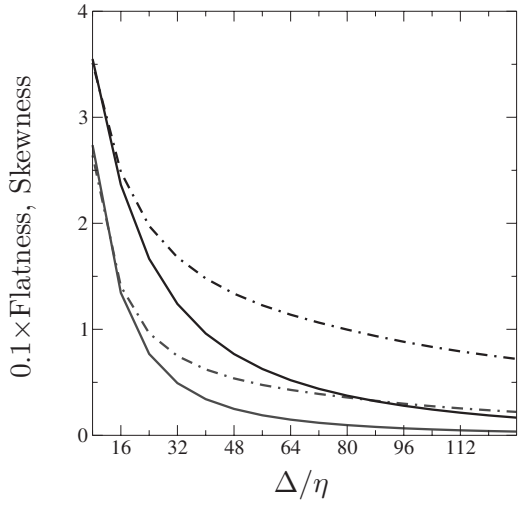

FIG. 14. Skewness (black) and flatness (gray) of the subfilter variance. The values of the flatness are divided by 10. Z_v (—) and $Z_{v,\mathrm{LED}}$ (–·–).

V. CONCLUSIONS

The subfilter scalar variance model was evaluated using the concept of optimal estimators. It appears more suitable to formulate a subfilter variance model by using the set of quantities of the dynamic variance model[7] than the set of variables of the scale-similarity model.[6] However, it was found that the main assumptions used in the dynamic Smagorinsky-type model formulation lead to large errors in the variance predictions. The dynamic model assumes that the same model coefficient can be applied at both the filter and the test filter levels. Moreover, it is assumed that the application of the test filter is equivalent to first applying the regular filter followed by a test filter. A Taylor-expansion analysis showed that this assumption is equivalent to neglecting a first-order term in the expansion $\widehat{\overline{Z}\overline{Z}}-\overline{\widehat{Z}}\overline{\widehat{Z}}$. Inclusion of higher-order expansion terms has led to a new dynamic model formulation. *A priori* tests using DNS of forced homogeneous isotropic turbulence showed that the new model substantially improves predictive accuracy.

ACKNOWLEDGMENTS

The authors gratefully acknowledge funding from NASA and the Air Force Office of Scientific Research.

[1] R. S. Rogallo and P. Moin, "Numerical simulation of turbulent flows," Annu. Rev. Fluid Mech. **16**, 99 (1984).
[2] M. Lesieur and O. Métais, "New trends in large-eddy simulations of turbulence," Annu. Rev. Fluid Mech. **28**, 45 (1996).
[3] C. Meneveau and J. Katz, "Scale-invariance and turbulence models for large-eddy simulation," Annu. Rev. Fluid Mech. **32**, 1 (2000).
[4] S. B. Pope, *Turbulent Flows* (Cambridge University Press, Cambridge, 2000).
[5] H. Pitsch, "Large-eddy simulation of turbulent combustion," Annu. Rev. Fluid Mech. **38**, 453 (2006).
[6] A. W. Cook and J. J. Riley, "A subgrid model for equilibrium chemistry in turbulent flows," Phys. Fluids **6**, 2868 (1994).
[7] C. D. Pierce and P. Moin, "A dynamic model for subgrid-scale variance and dissipation rate of a conserved scalar," Phys. Fluids **10**, 3041 (1998).
[8] K. Alvelius, "Random forcing of three-dimensional homogeneous turbulence," Phys. Fluids **11**, 1880 (1999).
[9] D. A. Donzis, K. R. Sreenivasan, and P. K. Yeung, "Scalar dissipation rate and dissipative anomaly in isotropic turbulence," J. Fluid Mech. **532**, 199 (2005).

[10]J. Jimenez and A. A. Wray, "On the characteristics of vortex filaments in isotropic turbulence," J. Fluid Mech. **373**, 255 (1998).
[11]C. Wall, B. J. Boersma, and P. Moin, "An evaluation of the assumed beta probability density function subgrid-scale model for large eddy simulation of nonpremixed, turbulent combustion with heat release," Phys. Fluids **12**, 2522 (2000).
[12]R. Deutsch, *Estimation Theory* (Prentice-Hall, Englewood Cliffs, 1965).
[13]A. Moreau, O. Teytaud, and J. P. Bertoglio, "Optimal estimation for large-eddy simulation of turbulence and application to the analysis of subgrid models," Phys. Fluids **18**, 105101 (2006).
[14]R. A. Clark, J. H. Ferziger, and W. C. Reynolds, "Evaluation of subgrid-scale models using an accurately simulated turbulent flow," J. Fluid Mech. **91**, 1 (1979).
[15]S. Liu, C. Meneveau, and J. Katz, "On the properties of similarity subgrid-scale models as deduced from measurements in a turbulent jet," J. Fluid Mech. **275**, 83 (1994).
[16]K. W. Bedford and W. K. Yeo, in *Large Eddy Simulation of Complex Engineering and Geophysical Flows*, edited by B. Galperin and S. A. Orszag (Cambridge University Press, New York, 1993).
[17]E. Pomraning and C. J. Rutland, "Dynamic one-equation nonviscosity large-eddy simulation model," AIAA J. **40**, 689 (2002).
[18]C. B. da Silva and J. C. F. Pereira, "Analysis of the gradient-diffusion hypothesis in large-eddy simulations based on transport equations," Phys. Fluids **19**, 1 (2007).
[19]D. K. Lilly, "A proposed modification of the germano subgrid-scale closure method," Phys. Fluids A **4**, 633 (1992).